

# Size and transparency influence diel vertical migration patterns in copepods.

Alex Barth        ?????        Joshua Stone

22 Mar 2023

## 1 Abstract

Diel vertical migration (DVM) is a widespread phenomenon in aquatic environments. The primary hypothesis explaining DVM is the visual predator evasion hypothesis, which suggests that zooplankton migrate to deeper waters to avoid detection during daylight. However, visual risk also depends on a copepod's morphology. In this study, we investigate hypotheses related to morphology and DVM: (H1) size increases visual risk and will increase DVM and (H2) copepod transparency will reduce visual risk and thus reduce DVM. Copepod images were collected across several cruises in the Sargasso Sea using an Underwater Vision Profiler 5. Copepod morphology was characterized from these images and a dimension reduction approach. The results show a clear relationship in which larger copepods have a larger DVM signal. Darker copepods appear to have a larger DVM signal, however only amongst the largest group of copepods. This suggest a complex relationship between copepod morphology and behavior.

## 18 **2 *Scientific Significance Statement***

19 Diel Vertical Migration is a widespread phenomenon across marine and freshwater systems.  
20 The predator evasion hypothesis suggests that DVM occurs as zooplankton attempt to escape  
21 visual predators. Yet, DVM itself is a costly and risky behavior. Thus, DVM should only  
22 occur when visual risk is high. Several studies have shown that copepod size influences the  
23 magnitude of DVM. However, an individual's visual risk may include traits beyond simply  
24 size. In this study, we utilize an in-situ imaging tool to reveal how copepod morphological  
25 traits influence DVM. Our findings show that both size and transparency influence DVM. This  
26 finding highlights that DVM is a complex behavior driven by copepod traits. Furthermore,  
27 this study exemplifies the ability of new technology to draw insights into plankton ecology.

## 28 **3 Introduction**

29 Diel vertical migration (DVM) is a wide spread phenomena with large consequences in ocean  
30 ecosystems. DVM is the process of pelagic organisms vertically moving in the water column on  
31 a daily basis, often travelling dozens to hundreds of meters (Bianchi and Mislan 2016). This  
32 large-scale event occurs across many taxa, from plankton to fish (Brierley 2014). However,  
33 DVM is particularly notable in zooplankton communities, whose migrations contribute sub-  
34 stantially to biogeochemical cycles (Steinberg and Landry 2017; Archibald et al. 2019; Siegel  
35 et al. 2023). Zooplankton communities, largely dominated by copepods (Turner 2004), will  
36 feed in surface layers of the ocean then migrate into deeper waters. Through this movement,

37 copepods actively transport carbon to depth. Additionally, Kelly et al. (2019) described  
38 zooplankton DVM to be a major component of mesopelagic food webs. Thus it is critically  
39 important to understand the drivers of DVM.

40 Predominantly, zooplankton DVM is the movement from deep waters at daytime to shallower  
41 waters at night (Hays 2003; Bianchi and Mislan 2016). The leading explanation for this  
42 pattern is the predator-avoidance hypothesis (Bandara et al. 2021). This hypothesis posits  
43 zooplankton evacuate the sunlit surface to evade visual predators then ascend at night to  
44 feed. However, the massive migration undertaken by these copepods is energetically expensive  
45 (Maas et al. 2018). Therefore, the visual predator evasion hypothesis implies that DVM is a  
46 result of visual risk exceeding migration costs. However, a copepod's visual risk to a visual  
47 predator depends morphological features (Aksnes and Utne 1997). Notably a copepod's size  
48 can increase visual detection. Several studies have documented that copepod size influences  
49 DVM magnitude (Hays et al. 1994; Aarflot et al. 2019). Presumably, a copepod's transparency  
50 will also influence DVM. Hays et al. (1994) reported that pigmentation explained variation in  
51 DVM frequency. However, few other studies have investigated this at length. One barrier to  
52 studying a relationship between copepod morphology and DVM is the difficulty of accurately  
53 recording traits.

54 In-situ imaging tools offer great potential to better describe copepod DVM. By directly observ-  
55 ing a copepod, new insights into their behavior and traits can be resolved (Ohman 2019). For  
56 example, Whitmore and Ohman (2021) used an in-situ imaging device to describe a relation-  
57 ship of copepod abundance with a particulate field rather than chlorophyll-a. Such findings

are facilitated by the fact imagery data records an individual's exact position. Additionally, a copepod's true appearance can be documented whereas net-collected organisms are often deformed or lacking color. Some studies have noted a copepod DVM with in-situ imagery data (Pan et al. 2018; Whitmore and Ohman 2021). However, direct tests of DVM-related hypotheses with such data have not been conducted.

In this study, we utilized in-situ imaging to evaluate how copepod morphological traits influence patterns. We specifically test the hypotheses that, (H1) size increases visual risk and will increase DVM and (H2) copepod transparency will reduce visual risk and thus reduce DVM. If these morphologically based hypotheses are true, then the larger and darker copepods will have the largest DVM signals.

## 4 Methods

### 4.1 CTD profiles and UVP imaging of copepods

Data were collected aboard the R/V Atlantic Explorer in collaboration with the Bermuda Atlantic Time-series Study (BATS) (Steinberg et al. 2001). In-situ images of plankton were acquired using an Underwater Vision Profiler (UVP5) (Picheral et al. 2010). The original sampling methodology and instrument specification followed details described in (Barth and Stone 2022). The UVP was attached to the CTD rosette and deployed intermittently on cruises to the Sargasso Sea from June 2019 - December 2021. Typical monthly cruises included ~13 profiles with average descents to 1200m (Supplemental Figure 1). In this study, we investigated

77 general trends in DVM by pooling together casts across multiple cruises. This approach is  
78 necessitated by the small sampling volume of the UVP and low abundance of plankton which  
79 requires aggregation of data to resolve trends (Barth and Stone 2022). While there was  
80 some variation between cruises (Supplemental Figure 2), this oligotrophic system is relatively  
81 consistent across seasons. Additionally, every cruise had an approximately equal number of  
82 day and night casts. Profiles were assigned to be day or night based on locally calculated  
83 nautical dawn and nautical dusk times using the R package `suncalc` 0.5.1.

84 The UVP records images of large particles ( $>600\mu\text{m}$  ESD). However, living particles are not  
85 reliably identifiable below 0.9 mm (Barth and Stone 2022). All recorded images were processed  
86 using Zooprocess (Gorsky et al. 2010), which provides several metrics related to size, grey  
87 value, and shape complexity. These features were then used to automatically sort images using  
88 Ecotaxa (Picheral et al.). All images were manually verified by the same trained taxonomist.  
89 In total, 294,913 images were recorded. Of these, 85.2% were images of debris or artefacts.  
90 The smallest identified copepod was 0.940mm ESD and the largest was 5.904mm ESD. Across  
91 all casts, copepods were the most common organism, composing 58.7% of all identified, living  
92 particles. In total, there were 4151 individual copepods images.

## 93 **4.2 Morphological Grouping**

94 The UVP automatically measures and collects several morphologically relevant parameters.  
95 To create relevant groups of copepods, a dimension reduction and clustering approach was  
96 used. Similar methods have been successfully utilized to provide novel insights to marine snow

97 (Trudnowska et al. 2021), copepod dynamics in the Arctic (Vilgrain et al. 2021), and temporal  
98 trends in phytoplankton communities (Sonnet et al. 2022). First, 18 morphologically relevant  
99 parameters were selected to be included in a principal Components Analysis (PCA), following  
100 (Vilgrain et al. 2021). Parameters can be described as relating to size (e.g. major axis, feret  
101 diameter, ESD), grey intensity (e.g. mean grey value), shape (e.g. elongation, symmetry), and  
102 shape complexity (e.g. fractal dimension). The PCA was weighted by the volume sampled in a  
103 1-m depth bin for each observation. This approach provides a correction for the UVP’s variable  
104 descent speed which can cause duplicate imaging of individuals. While this phenomena has  
105 a minor impact on overall results (Barth and Stone 2022), we used the weighted approach to  
106 assure that no individual features were overrepresented. All morphological descriptors were  
107 scaled and centered prior to inclusion in the analysis. The model was constructed using the  
108 R package **FactoMineR 2.7**. principal components were deemed to be significant if their  
109 eigenvalues were greater than 1. This approach yielded 4 PCs which described 87.3% of the  
110 total variation in morphological parameters, with 34.5% and 26.5% in the first two components  
111 respectively. This four principal component space provides a “morphospace” to characterize  
112 copepods.

113 To address our morphology-DVM hypotheses, we constructed discrete morphological groups  
114 based on the first two principal components. Groups along each of the principal components  
115 were defined as low (below 25th percentile), mid (25th-75th percentile) and high (greater than  
116 75th percentile). To address the size-dependent hypothesis (H1), groups were assigned as low,  
117 mid, or high along PC1. Then to assess if color/transparency was a secondary factor (H2),

118 within each PC1 group, PC2 groups were constructed as low, mid, or high. In total, this  
119 created 9 groups (e.g. Low PC1-Low PC2, Low P1-mid PC2, etc).

## 120 **4.3 Copepod vertical structure & DVM**

### 121 **4.3.1 Vertical distribution of copepods**

122 Copepods in this system are well documented to undergo DVM (Steinberg et al. 2000; Schnet-  
123 zer and Steinberg 2002; Maas et al. 2018) However, there have not been direct measurements  
124 of DVM with in situ imaging data. First, to assess which portion of the water column cope-  
125 pods were utilizing for DVM, we visualized the average vertical structure. The concentration  
126 of each morphological group (based on PC1 and PC2) were calculated in 20m depth bins for  
127 each UVP profile. These binned-profiles were then averaged together based on time of day.

### 128 **4.3.2 Weighted mean depth variability**

129 Weighted mean depth (WMD) is a common metric to describe vertical structure and DVM in  
130 zooplankton (Ohman et al. 2002; Ohman and Romagnan 2016; Aarflot et al. 2019). However,  
131 with in-situ imagery, this approach presents a few challenges. WMD cannot be calculated  
132 individually for each profile then averaged because each profile had a different descent depth.  
133 Additionally, the small and uneven sampling volume of the UVP can make single casts inaccu-  
134 rate. Yet, understanding variation around the WMD is necessary to compare DVM strength  
135 across groups. Here, we introduce a depth-bin constrained bootstrap approach to define WMD

136 with a 95% confidence interval. To do this, the concentration of each group, was calculated  
 137 in 20m depth bin for each profile. Then all profiles from the same time of day were ‘pooled’.  
 138 This provides a distribution of concentrations in each depth-bin. Traditional bootstrapping  
 139 randomly samples, with replacement, all observations. With vertically structured data how-  
 140 ever, full random sampling would bias estimates towards the surface. To avoid this, samples  
 141 were “bin-constrained” such that for each iteration, a random observation was sampled within  
 142 each depth bin, then replaced for the next iteration. A maximum depth was set to 600m, as  
 143 it is unlikely that typical copepod DVM extends beyond this point. This approach effectively  
 144 created a random profile by resampling a concentration,  $conc^*$ , from each depth bin,  $d$ . This  
 145 profile then was used to calculate a bootstrapped weighted mean depth,  $WMD^*$ . This was  
 146 done for each morphological group  $g$ , at each time of day  $t$ .

$$WMD_{g,t}^* = \sum_i^{N=60} \frac{d_i(conc_{i,g,t}^*)}{\sum_i^{N=60} conc_{i,g,t}^*}$$

147 The distribution of  $WMD_{g,t}^*$  then was used to calculate a bootstrapped mean and 95% con-  
 148 fidence interval. The 95% CIs could be compared between times of day and morphological  
 149 groups to assess the strength of DVM. Using PC1 to assess size, the WMD was compared  
 150 between the three PC1-groups by percentile level. Then to assess the effect of transparency  
 151 the WMD was compared between PC2-groups within each PC1-grouping. A larger signal of  
 152 DVM would be evident by a clearly deeper (non-overlapping 95% CI) daytime WMD.



## 4.4 Data availability

All data and code are made available via ([https://github.com/TheAlexBarth/DVM\\_Migration-Morphology](https://github.com/TheAlexBarth/DVM_Migration-Morphology)). All supplemental figures, tables, and analyses are hosted on a public static site ([https://thealexbarth.github.io/DVM\\_Migration\\_Morphology](https://thealexbarth.github.io/DVM_Migration_Morphology)).

## 5 Results

### 5.1 Morphological Groups

The PCA revealed four major axis of variability (Figure 1). The first axis (PC1, 34.23% of variability) was largely explained by increasing values related to size, such as perimeter (loading score = 0.927) and feret diameter (loading score = 0.910). The second axis (PC2, 27.24% of variability) can be interpreted as a gradient of transparent to dark individuals. PC2 was largely anticorrelated with mean grey value (higher values indicate a more transparent individual) (loading score = -0.920). As noted in the methods, PC3 and PC4 were both related to the orientation of the copepod and the appendage visibility respectively (Supplemental Figure 3).

The morphological groupings were assigned along PC1 as low, mid and high. Then along PC2, groups were assigned within each PC1-group (Figure 1). To confirm the morphospace grouping resulted in ecologically relevant categories, the morphological groups were compared against known copepod metrics. Across all PC1-groups, there was a clear difference in feret diameter.

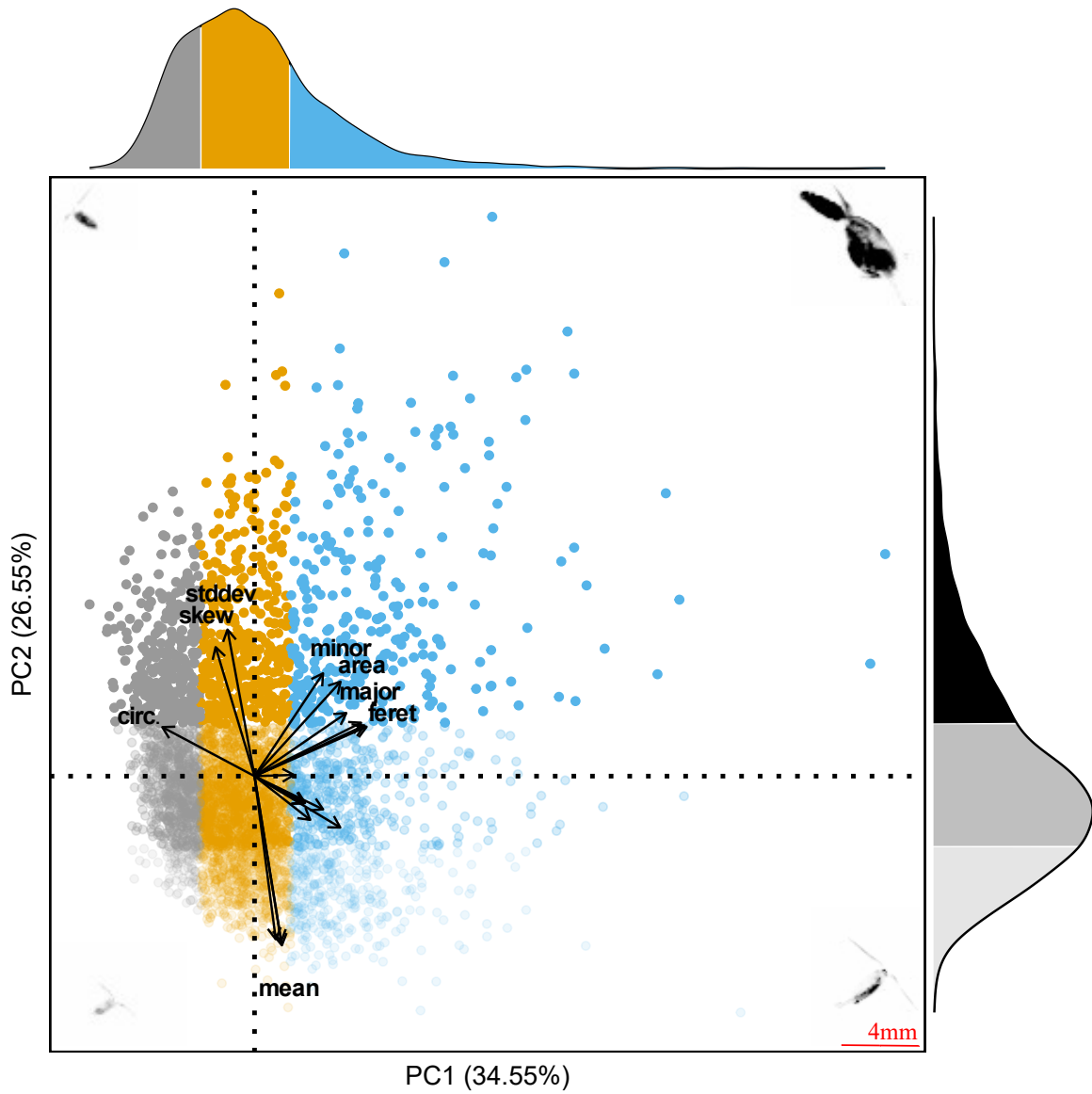


Figure 1: First two principal components of the morphospace. Proportion of variance explained by the two axis is . Each point represents an individual copepod. The color and transparency of each point corresponds to the morphological groups based on percentile along each axis. Marginal distribution display the proportion of observations in each group. Representative vignettes of copepods are shown in the corners corresponding to their place in the morphospace. 4mm scale bar in the bottom right is shown for the vignettes.

171 The median feret diameter of the low group was 1.97mm. The median feret diameter of the  
172 mid and high groups were 2.84mm and 4.83mm, respectively (Figure 2A). All groups were  
173 significantly different from one another (Dunn Kruskal-Wallace test,  $p < 0.001$ ). PC2 groups  
174 as a whole were also significantly different from one another (Dunn Kruskal-Wallace test,  $p <$   
175  $0.001$ ). However, within each PC2-group, there was a clear tendency for larger copepods (high  
176 PC1 group) to be more transparent (Figure 2B).

## 177 **5.2 Vertical Profiles of Morphological Groups**

178 For all groups, the 20m-binned profiles show a notable structure. While copepods were ob-  
179 served throughout the mesopelagic (Supplemental Figure 4), the majority of day/night differ-  
180 ences were observed above 600m (Figure 3). For all morphological groups, there was a peak in  
181 nighttime concentration in the lower epipelagic (50m-200m). Similarly, there was a decrease  
182 in average daytime concentration over the same region. This pattern is particularly apparent  
183 for the groups which are mid and high on both PCs (Figure 3B, C, E, F). Across all groups,  
184 both average daytime and nighttime concentration were low in the upper mesopelagic (200m-  
185 300m). Then, there was a peak in average daytime concentration in the depth bins in the  
186 mid-mesopelagic (400m-600m).

## 187 **5.3 Weighted mean depth analysis**

188 The bin-constrained bootstrap approach provided a direct method to compare DVM between  
189 groups. Size (PC1) had a clear effect on DVM magnitude. First, for all PC1 groups, daytime

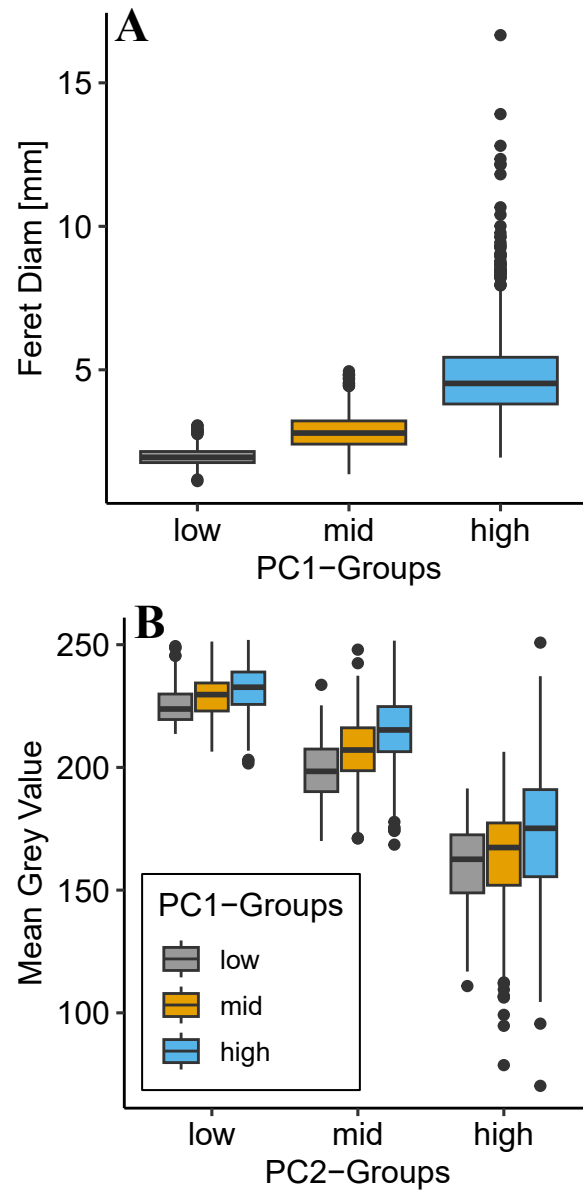


Figure 2: Comparison of morphological groups to relevant parameters. Groups were constructed along principal components with low as below 25th percentile, mid as 25th-50th percentile, and high as above 75th percentile. (A) PC1 groups are significantly different along feret diameter and display a clear trend for size. (B) PC2 groups are significantly different in terms of mean grey value. Note that a low mean grey value indicates a darker copepod.

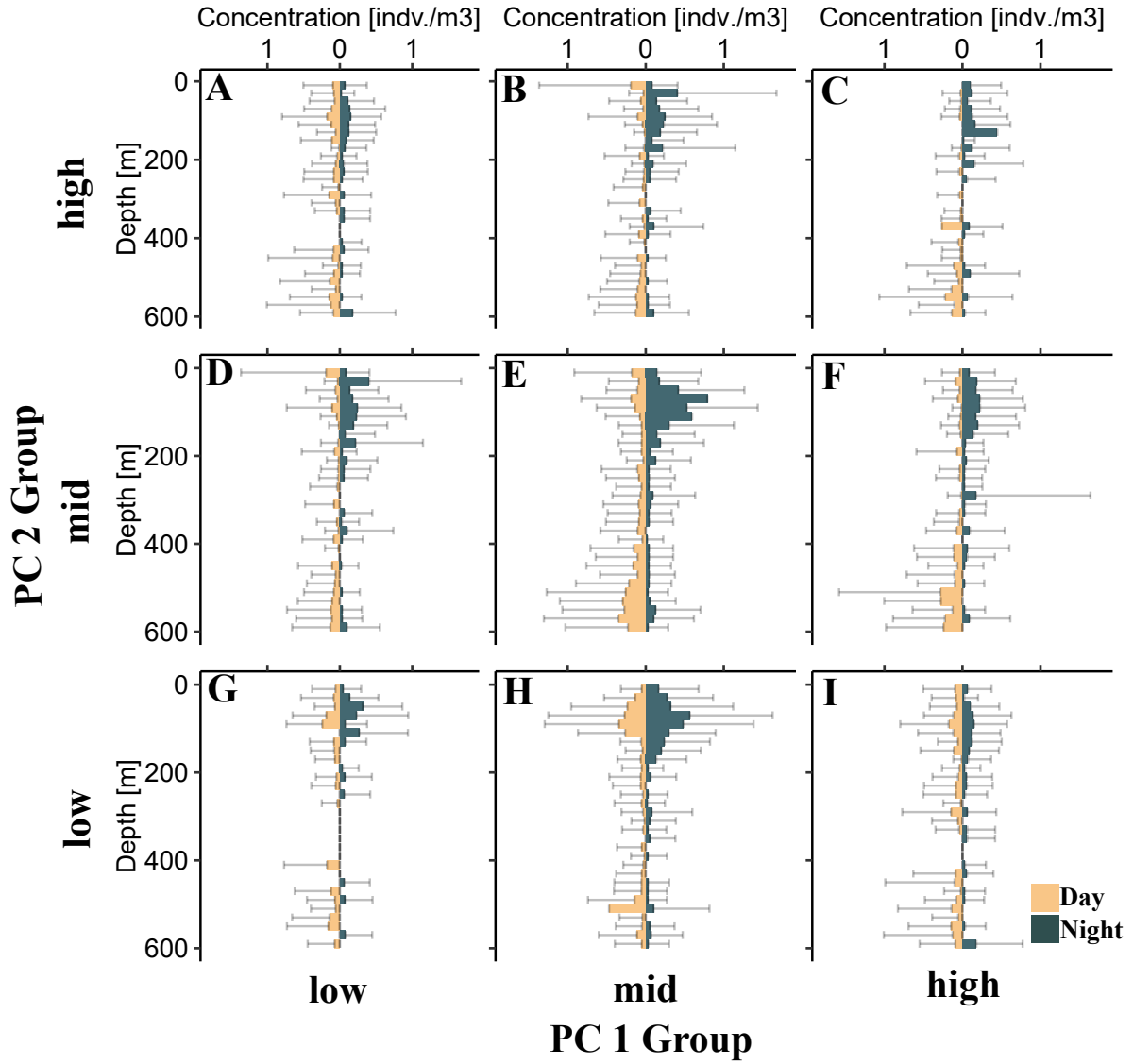


Figure 3: Average vertical profile of different copepod morphological groups. Bars display average concentration in a 20m depth bin. On each panel, left-side bars correspond to daytime while right-side bars correspond to nighttime. Standard deviation is shown for each 20m depth bin. Each panel corresponds to a morphological group along PC1 (size axis) and PC2 (transparency axis). (A) low PC1, high PC2; (B) mid PC1, high PC2; (C) high PC1, high PC2; (D) low PC1, mid PC2; (E) mid PC1, mid PC2; (F) high PC1, mid PC2; (G) low PC1, low PC2; (H) mid PC1, low PC2; (I) high PC1, low PC2

WMD 95% bootstrapped confidence intervals (95% CIs) were deeper and non-overlapping with the nighttime 95% CIs (Figure 4). This indicates a clear DVM pattern. However, the differences in day and night CIs varied between morphological groups. All PC1 groups had a similar, overlapping nighttime 95% CI in the lower epipelagic (~145m - ~200m). However, there was a clear difference in the depth of the daytime 95% CIs. The small (low PC1) group had the shallowest 95% CI (235.2m-296.0m). The mid PC1 group's daytime 95% CI was slightly deeper (309.0m-347.3m). The large (high PC1) group daytime 95% CI was even lower (352.3m-405.0m).

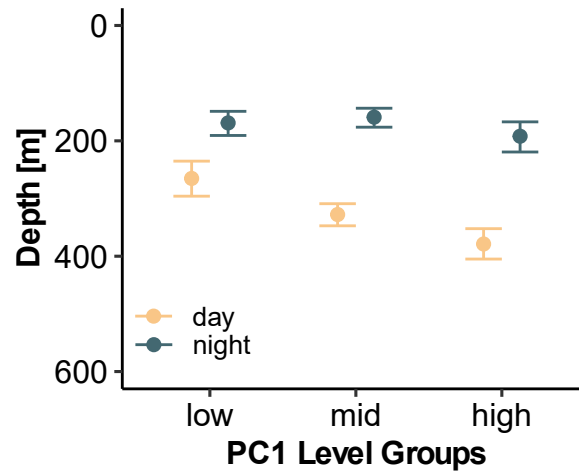


Figure 4: Mean bootstrapped weighted mean depth and 95% confidence intervals for copepods of different morphological groups. Low, mid, and high groups correspond to the different percentiles along PC1 from the morphospace. PC1 largely is explained by size metrics, with higher scores indicating a larger copepod.

When considering the influence of transparency (PC2) on DVM magnitude, we compared PC2 groups within their PC1 grouping. This approach was warranted because of the tendency for size to have a slight effect on transparency (Figure 2). At this level of comparison, there were several notable trends. For the smaller copepods (low PC1), once the data were split

202 into PC2 groups, the wider 95% CIs indicate little to no DVM signal. Generally, the daytime  
 203 95% CIs and nighttime 95% CIs are overlapping or near-overlapping (Figure 5A). With mid  
 204 sized copepods, there was a clear DVM signal. However, all PC2 groups appeared to have  
 205 a similar DVM magnitude with each group's daytime 95% CIs overlapping with each other  
 206 (Figure 5B). There was a difference in DVM magnitude across PC2 groups within the largest  
 207 copepods. The more transparent copepods (low PC2 group) showed no DVM signal, with a  
 208 shallow daytime WMD. However, the darker copepods (mid and high PC2 groups) had deeper  
 209 daytime WMDs (Figure 5c).

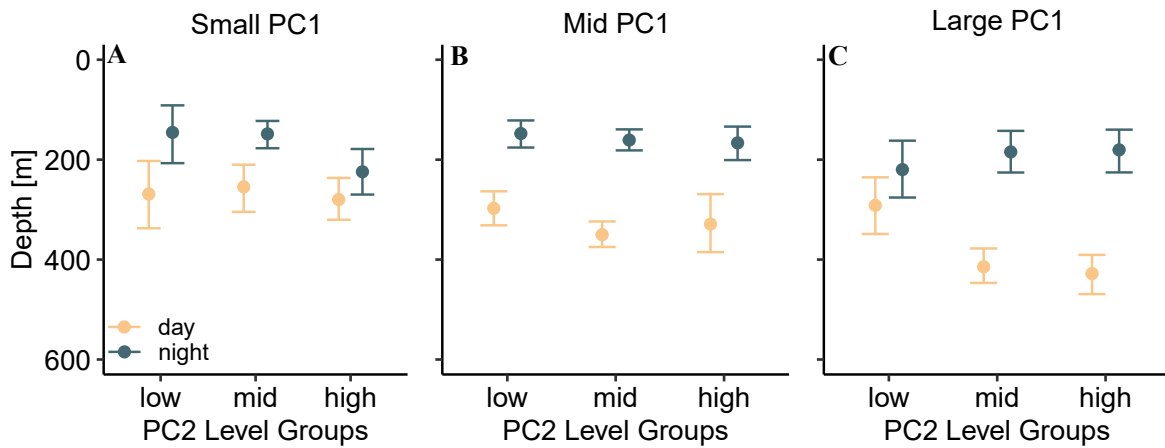


Figure 5: Mean bootstrapped weighted mean depth and 95% confidence intervals shown by copepod morphological groups along PC2 (transparency). Each panel represents a different size group of copepods (PC1 groups).

## 6 Discussion

### 6.1 Copepod morphospace

In this study, we built on methods for describing morphospaces from similar in-situ imaging studies (Vilgrain et al. 2021; Trudnowska et al. 2021; Sonnet et al. 2022). The PCA-defined morphospace with the present data aligns well with the prior applications. Interestingly, the morphospace defined on Arctic copepods by Vilgrain et al. (2021) is extremely similar to the morphospace in this study. The proportion of morphological variation explained by each of the four principle components are extremely close between these two studies. It is possible that this is an artifact of the similarity of input data. Given the UVP has a limited range of observable size classes (Picheral et al. 2010), only copepods above a certain size were fed into both PCAs. Nonetheless, it is striking that the two morphospaces are similar considering the vastly different community compositions between the Arctic ocean and subtropical gyres (Soviadan et al. 2022).

### 6.2 Morphology and DVM

The pattern of DVM described in this study is consistent with the general DVM pattern (Bianchi and Mislán 2016; Bandara et al. 2021). The average vertical profiles display a clear day/night difference (Figure 3). In each 20m depth bin, there was large variation, often exceeding the average concentration. This large variation however, was expected. There can be considerable variation between UVP estimates of zooplankton abundance (Barth and



Stone 2022). Additionally, in this study we pooled casts across multiple seasons. Variability in copepod DVM has been described across seasons (Whitmore and Ohman 2021). While seasonal variability in DVM is in an interesting question in the Sargasso Sea, the nature of our dataset did not lend itself to this investigation. However, despite the need to pool UVP casts across, the signal of DVM was still observable. Previous studies using in-situ imaging have also noted a signal of DVM with copepods (Pan et al. 2018; Whitmore and Ohman 2021). Yet due to small and uneven sampling, it can be a challenge to quantify DVM using in-situ imaging. As presented in this paper, bin-constrained bootstrapping offers a robust method to quantify WMD and investigate DVM hypotheses.

Copepod size had a clear effect in which larger copepods migrated further. This finding is consistent with several studies which have documented a size-dependent relationship for copepod DVM (Ohman and Romagnan 2016; Aarflot et al. 2019; Pinti et al. 2019). Ohman and Romagnan (2016) noted that moderate-size copepods had the largest migrations. While this may seem contradictory to the present study, the difference between study systems needs to be taken into account. The copepods described in the large (high PC1) group had a mean feret diameter of nearly 5mm. Conversely, in Ohman and Romagnan (2016)’s study the “moderate” copepods ranged from 4mm-6mm. An effect of transparency on copepod DVM was only observed in the large copepod group. The large but more transparent copepods (low PC2, high PC1) did not have a detectable DVM signal. Yet the darker copepods (mid and high PC2) had a large DVM signal. Hays (2003) described that copepod pigmentation could explain increased DVM with small (<1mm) copepods. The lack of a transparency effect for the mid- and low

PC1 groups in our study is surprising. One possibility is that the small, transparent copepods were not well sampled by the UVP (Figure 2). Alternatively, some copepods which do not migrate may have pigmentation to avoid damage from UV radiation. While well documented, predator avoidance may not always be the primary selective pressure on copepod traits. For example, if the costs of migration are too large for some copepods, they will remain near the surface. However, these copepods then are exposed to UV light and may increase pigmentation to reduce damage. Likely the relationship between color and DVM is the result of a delicate balance of minimizing multiple ecological and biological risks (Hansson 2004; Hylander et al. 2014). Nonetheless, our results provide some support for the relationship between copepod color and DVM magnitude. Grey-value in UVP-imaged copepods can be indicative of many features beyond simply pigmentation, notably egg-sacs and gut contents (Vilgrain et al. 2021). Such characteristics vary much more between individuals and can have varied influences on DVM (PEARRE Jr. 2003).

## References

- Aarflot, J. M., D. L. Aksnes, A. F. Opdal, H. R. Skjoldal, and Ø. Fiksen. 2019. Caught in broad daylight: Topographic constraints of zooplankton depth distributions. *Limnology and Oceanography* **64**: 849–859. doi:[10.1002/lno.11079](https://doi.org/10.1002/lno.11079)
- Aksnes, D. L., and A. C. W. Utne. 1997. A revised model of visual range in fish. *Sarsia* **82**: 137–147. doi:[10.1080/00364827.1997.10413647](https://doi.org/10.1080/00364827.1997.10413647)
- Archibald, K. M., D. A. Siegel, and S. C. Doney. 2019. Modeling the Impact of Zooplank-

ton Diel Vertical Migration on the Carbon Export Flux of the Biological Pump. *Global Biogeochemical Cycles* **33**: 181–199. doi:[10.1029/2018GB005983](https://doi.org/10.1029/2018GB005983)

Bandara, K., Ø. Varpe, L. Wijewardene, V. Tverberg, and K. Eiane. 2021. Two hundred years of zooplankton vertical migration research. *Biological Reviews* **96**: 1547–1589. doi:[10.1111/brv.12715](https://doi.org/10.1111/brv.12715)

Barth, A., and J. Stone. 2022. [Comparison of an in situ imaging device and net-based method to study mesozooplankton communities in an oligotrophic system.](#) *Frontiers in Marine Science* **9**.

Bianchi, D., and K. a. S. Mislan. 2016. Global patterns of diel vertical migration times and velocities from acoustic data. *Limnology and Oceanography* **61**: 353–364. doi:[10.1002/lno.10219](https://doi.org/10.1002/lno.10219)

Brierley, A. S. 2014. Diel vertical migration. *Current Biology* **24**: R1074–R1076. doi:[10.1016/j.cub.2014.08.054](https://doi.org/10.1016/j.cub.2014.08.054)

Gorsky, G., M. D. Ohman, M. Picheral, and others. 2010. Digital zooplankton image analysis using the ZooScan integrated system. *Journal of Plankton Research* **32**: 285–303. doi:[10.1093/plankt/fbp124](https://doi.org/10.1093/plankt/fbp124)

Hansson, L.-A. 2004. Plasticity in Pigmentation Induced by Conflicting Threats from Predation and Uv Radiation. *Ecology* **85**: 1005–1016. doi:[10.1890/02-0525](https://doi.org/10.1890/02-0525)

Hays, G. C. 2003. [A review of the adaptive significance and ecosystem consequences of zooplankton diel vertical migrations.](#) Springer Netherlands. 163–170.

Hays, G. C., C. A. Proctor, A. W. G. John, and A. J. Warner. 1994. Interspecific differences in the diel vertical migration of marine copepods: The implications of size, color, and mor-

292 phology. *Limnology and Oceanography* **39**: 1621–1629. doi:[10.4319/lo.1994.39.7.1621](https://doi.org/10.4319/lo.1994.39.7.1621)

293 Hylander, S., J. C. Grenvald, and T. Kiørboe. 2014. Fitness costs and benefits of ultra-  
 294 violet radiation exposure in marine pelagic copepods. *Functional Ecology* **28**: 149–158.  
 295 doi:[10.1111/1365-2435.12159](https://doi.org/10.1111/1365-2435.12159)

296 Kelly, T. B., P. C. Davison, R. Goericke, M. R. Landry, M. D. Ohman, and M. R. Stukel. 2019.  
 297 [The importance of mesozooplankton diel vertical migration for sustaining a mesopelagic](#)  
 298 [food web](#). *Frontiers in Marine Science* **6**.

299 Maas, A. E., L. Blanco-Bercial, A. Lo, A. M. Tarrant, and E. Timmins-Schiffman. 2018. Vari-  
 300 ations in copepod proteome and respiration rate in association with diel vertical migration  
 301 and circadian cycle. *The Biological Bulletin* **235**: 30–42. doi:[10.1086/699219](https://doi.org/10.1086/699219)

302 Ohman, M. D. 2019. A sea of tentacles: optically discernible traits resolved from planktonic  
 303 organisms in situ H. Browman [ed.]. *ICES Journal of Marine Science* **76**: 1959–1972.  
 304 doi:[10.1093/icesjms/fsz184](https://doi.org/10.1093/icesjms/fsz184)

305 Ohman, M. D., and J.-B. Romagnan. 2016. Nonlinear effects of body size and optical at-  
 306 tenuation on Diel Vertical Migration by zooplankton. *Limnology and Oceanography* **61**:  
 307 765–770. doi:[10.1002/lno.10251](https://doi.org/10.1002/lno.10251)

308 Ohman, M. D., J. A. Runge, E. G. Durbin, D. B. Field, and B. Niehoff. 2002. On birth and  
 309 death in the sea. *Hydrobiologia* **480**: 55–68. doi:[10.1023/A:1021228900786](https://doi.org/10.1023/A:1021228900786)

310 Pan, J., F. Cheng, and F. Yu. 2018. [The diel vertical migration of zooplankton in the hypoxia](#)  
 311 [area observed by video plankton recorder](#). *IJMS Vol.47(07)* [July 2018].

312 PEARRE Jr., S. 2003. Eat and run? The hunger/satiation hypothesis in verti-  
 313 cal migration: history, evidence and consequences. *Biological Reviews* **78**: 1–79.

doi:[10.1017/S146479310200595X](https://doi.org/10.1017/S146479310200595X)

Picheral, M., S. Colin, and J.-O. Irisson. [EcoTaxa, a tool for the taxonomic classification of images.](#)

Picheral, M., L. Guidi, L. Stemann, D. M. Karl, G. Iddaoud, and G. Gorsky. 2010. The Underwater Vision Profiler 5: An advanced instrument for high spatial resolution studies of particle size spectra and zooplankton. *Limnology and Oceanography: Methods* **8**: 462–473. doi:[10.4319/lom.2010.8.462](https://doi.org/10.4319/lom.2010.8.462)

Pinti, J., T. Kiørboe, U. H. Thygesen, and A. W. Visser. 2019. Trophic interactions drive the emergence of diel vertical migration patterns: A game-theoretic model of copepod communities. *Proceedings of the Royal Society B: Biological Sciences* **286**: 20191645. doi:[10.1098/rspb.2019.1645](https://doi.org/10.1098/rspb.2019.1645)

Schnetzer, A., and D. K. Steinberg. 2002. Active transport of particulate organic carbon and nitrogen by vertically migrating zooplankton in the Sargasso Sea. *Marine Ecology Progress Series* **234**: 71–84. doi:[10.3354/meps234071](https://doi.org/10.3354/meps234071)

Siegel, D. A., T. DeVries, I. Cetinić, and K. M. Bisson. 2023. Quantifying the ocean’s biological pump and its carbon cycle impacts on global scales. *Annual Review of Marine Science* **15**: null. doi:[10.1146/annurev-marine-040722-115226](https://doi.org/10.1146/annurev-marine-040722-115226)

Sonnet, V., L. Guidi, C. B. Mouw, G. Puggioni, and S.-D. Ayata. 2022. Length, width, shape regularity, and chain structure: time series analysis of phytoplankton morphology from imagery. *Limnology and Oceanography* **67**: 1850–1864. doi:[10.1002/lno.12171](https://doi.org/10.1002/lno.12171)

Soviadan, Y. D., F. Benedetti, M. C. Brandão, and others. 2022. Patterns of mesozooplankton community composition and vertical fluxes in the global ocean. *Progress in Oceanography*

336       **200**: 102717. doi:[10.1016/j.pocean.2021.102717](https://doi.org/10.1016/j.pocean.2021.102717)

337 Steinberg, D. K., C. A. Carlson, N. R. Bates, S. A. Goldthwait, L. P. Madin, and A. F. Michaels.

338       2000. Zooplankton vertical migration and the active transport of dissolved organic and

339       inorganic carbon in the Sargasso Sea. *Deep Sea Research Part I: Oceanographic Research*

340       Papers **47**: 137–158. doi:[10.1016/S0967-0637\(99\)00052-7](https://doi.org/10.1016/S0967-0637(99)00052-7)

341 Steinberg, D. K., C. A. Carlson, N. R. Bates, R. J. Johnson, A. F. Michaels, and A. H.

342       Knap. 2001. Overview of the US JGOFS Bermuda Atlantic Time-series Study (BATS):

343       a decade-scale look at ocean biology and biogeochemistry. *Deep Sea Research Part II:*

344       Topical Studies in Oceanography **48**: 1405–1447. doi:[10.1016/S0967-0645\(00\)00148-X](https://doi.org/10.1016/S0967-0645(00)00148-X)

345 Steinberg, D. K., and M. R. Landry. 2017. Zooplankton and the ocean carbon cycle. *Annual*

346       Review of Marine Science **9**: 413–444. doi:[10.1146/annurev-marine-010814-015924](https://doi.org/10.1146/annurev-marine-010814-015924)

347 Trudnowska, E., L. Lacour, M. Ardyna, A. Rogge, J. O. Irisson, A. M. Waite, M. Babin, and

348       L. Stemann. 2021. Marine snow morphology illuminates the evolution of phytoplankton

349       blooms and determines their subsequent vertical export. *Nature Communications* **12**: 2816.

350       doi:[10.1038/s41467-021-22994-4](https://doi.org/10.1038/s41467-021-22994-4)

351 Turner, J. 2004. The importance of small planktonic copepods and their roles in pelagic marine

352       food webs,.

353 Vilgrain, L., F. Maps, M. Picheral, M. Babin, C. Aubry, J.-O. Irisson, and S.-D. Ayata.

354       2021. Trait-based approach using in situ copepod images reveals contrasting ecological

355       patterns across an Arctic ice melt zone. *Limnology and Oceanography* **66**: 1155–1167.

356       doi:[10.1002/lno.11672](https://doi.org/10.1002/lno.11672)

357 Whitmore, B. M., and M. D. Ohman. 2021. Zooglider-measured association of zooplank-

358      ton with the fine-scale vertical prey field. *Limnology and Oceanography* **66**: 3811–3827.  
359      doi:[10.1002/lno.11920](https://doi.org/10.1002/lno.11920)